JACS
JOURNAL OF THE AMERICAN CHEMICAL SOCIETY

ARTICLE

pubs.acs.org/JACS

Chemical and Electrochemical Dimerization of BODIPY Compounds: Electrogenerated Chemiluminescent Detection of Dimer Formation

Alexander B. Nepomnyashchii,[†] Martin Bröring,[‡] Johannes Ahrens,[‡] and Allen J. Bard*[,†]

[†]Chemistry and Biochemistry Department, The University of Texas at Austin, Austin, Texas, 78712, United States

[‡]Institut für Anorganische und Analytische Chemie, Technische Universität Carolo-Wilhelmina, Hagenring 30, 38106 Braunschweig, Germany

Supporting Information

ABSTRACT: The electrochemistry of several difluoroboradiaza-*s*-indacene (BODIPY) compounds lacking substituent groups in the *meso* (8)- and/or 3 (α)-positions was investigated. Chemical and electrochemical dimerization was demonstrated, and the dimerization depended on the character of substitution. The chemical dimerization was achieved by oxidative coupling using $FeCl_3$ in CH_2Cl_2 at 0 °C. The electrochemical dimerization proceeded via anodic oxidation to the radical cation and monitored by both cyclic voltammetry (CV) and electrogenerated chemiluminescence (ECL). An available open 3-position was important for the formation of the dimer. The resulting 3,3′-dimer produced a second peak in the CV oxidation and also the appearance of a longer wavelength ECL peak at 656 nm, which is considerably shifted from the parent peak at 532 nm. No dimerization was seen for BODIPY molecules in which only the *meso* 8-position was unsubstituted, either by chemical or electrochemical means, demonstrating that dimerization occurs at position 3.

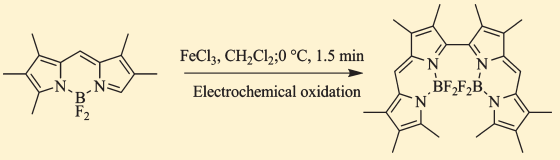

1. INTRODUCTION

Difluoroboradiaza-*s*-indacene (BODIPY) compounds are of interest as laser dyes, for biolabeling, and for photosensitization, since they show good photoluminescence and stability and can be tuned across a wide wavelength region (Scheme 1).[1−5] The compounds are of interest in electrochemical[6−13] and electrogenerated chemiluminescence (ECL) applications[6−10] and often show behavior in aprotic media analogous to the widely studied aromatic hydrocarbons.

The radical ions formed by one-electron transfer reactions are stable when the α, β and *meso* positions, which are susceptible to nucleophilic or electrophilic attack, are blocked. There have been many studies describing different ways of synthesizing BODIPY compounds with the aim of achieving the optimal synthesis conditions and high yield.[1] BODIPY compounds can also form dimers and other more branched units. Oxidative or reductive coupling can be used to obtain BODIPY dimers and larger structures. We report here a study of dimerization of the BODIPY dyes by both chemical and electrochemical oxidative coupling reactions for two compounds (Scheme 2) named with the indicated unsubstituted positions as **1**(×3,8) and **2**(×8) to produce the dimer coupled in the α-position, the 3,3′-dimer. This study is unique in its ability to compare dimerization via electrochemical oxidation and through chemical means to produce the same product.

Chemical dimerization was carried out by oxidative coupling using $FeCl_3$ in CH_2Cl_2 at 0 °C. $FeCl_3$ has been used previously as an oxidant for porphyrins[14−16] and is also a promising candidate for the dimerization of the BODIPY compounds.[17,18]

Scheme 1. Numbering of Positions in BODIPY Compounds[1]

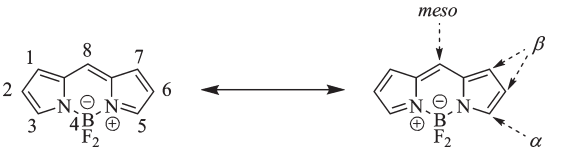

Electrochemistry can also be used for the coupling reactions.[19−21] Its advantage compared with the chemical methods is the more precise control of the oxidation potentials necessary to achieve coupling, with the potential of obtaining a higher yield of the product and lack of formation of products of the oxidant. Electrochemical dimerization by oxidative and reductive coupling reactions has been widely studied.[22−31] For example, electrohydrodimerization of activated olefins, most importantly acrylonitrile, by the hydrodimerization process is of importance as a commercial process for the production of the adiponitrile.[22−24] Numerous studies have been carried out to elucidate the dimerization mechanism and determine kinetic parameters for the reactions by using cyclic voltammetry (CV),[25−31,34−37] scanning electrochemical microscopy,[32,33] electron spin resonance,[27−29] and ECL.[34−37]

ECL coupled with CV is a useful tool for the rapid identification of the dimerization products and the mechanism of the coupling reactions and has been widely used in studies of the

Received: August 15, 2011
Published: October 24, 2011

Scheme 2. Chemical Structure of the (a) 1(×3,8), (b) 2(×8) and (c) 3,3′-Dimer

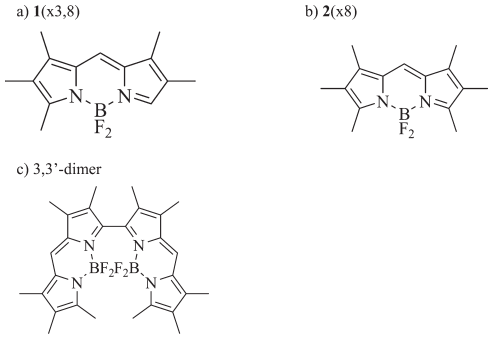

properties of the organic compounds. Details of ECL are discussed in many reviews and monographs[38] and will not be discussed here. ECL reactions can generate dimers electrochemically either during annihilation or by using a coreactant.[34−37] The necessary condition is the presence of a unique coupling reaction of an electrogenerated species. Debad et al. showed the possibility for the anodic coupling of the fluoranthene derivatives.[34,35] Fabrizio et al. showed production of the dimer from fluoranthene derivatives with peroxidisulfate as a coreactant.[36] Similar results were obtained by Lee et al., where the appearance of a longer wavelength emission in aqueous solutions for the oxidation of heptamine dyes in the presence of tripropylamine, assigned to the formation of the dimer.[37] Thus, the appearance of an additional (second) anodic peak and an additional ECL peak provides evidence for the formation of dimer, whereas the appearance of only the ECL peak for the monomer provides evidence of stability of the radical ion or its very slow dimerization. ECL studies of the unsubstituted BODIPY monomers can provide quick, independent and fast monitoring for the production of the coupling products, which can be important in synthesis of the biolabeling materials, as these compounds can be modified with active groups that can forms bonds with lipids, proteins, nucleic acids.[1]

2. EXPERIMENTAL SECTION

2.1. Chemical Synthesis and Characterization of BODIPY Dyes. Compounds **1**(×3,8) and **2**(×8)[39] were prepared from the corresponding dipyrrin hydrobromides[40] according to standard procedures. CH_2Cl_2 was dried by standard procedures and distilled from an appropriate drying agent. All reagents were purchased from commercial sources (Sigma-Aldich) and used as received. NMR spectra were obtained with a Bruker DRX 400 spectrometer. Chemical shifts (δ) are given in ppm relative to residual protio solvent resonances (^{1}H, ^{13}C NMR spectra) or to external standards ($BF_3 \cdot Et_2O$ for ^{11}B and $CFCl_3$ for ^{19}F NMR spectra). High-resolution ESI mass spectrum was recorded with a QStar Pulsar i.

*Preparation of 3,3′-Dimer (**3**).* Anhydrous $FeCl_3$ (74 mg, 0.458 mmol) was added to an ice bath cooled solution of 1,2,3,6,7-pentamethyl-4,4-difluoro-4-bora-3*a*,4*a*-diaza-*s*-indacene (**1**) (60 mg, 0.229 mmol) in dry CH_2Cl_2 (10 mL). The orange solution rapidly turned deep red. After 1.5 min the reaction was quenched by addition of MeOH (20 mL). The organic phase was washed with H_2O (2 × 50 mL), dried over Na_2SO_4 and concentrated to dryness on a rotary evaporator. The solid residue was separated by column chromatography on silica, first the residual educt was eluted with CH_2Cl_2/*n*-pentane = 1:1 as an orange fraction of yellowish green fluorescence (29 mg, 49% of recovered adduct). Then the product was eluted with CH_2Cl_2 as a red violet fraction with intensively red fluorescence and concentrated to a dirty violet solid with a green sheen.

Yield: 30 mg, 50%. ^{1}H NMR (400 MHz, CD_2Cl_2): δ = 7.17 (s, 2H; 8/8′-C*H*), 2.37 (s, 6H; CH_3), 2.26 (s, 6H; CH_3), 2.19 (s, 6H; CH_3), 1.93 (s, 6H; CH_3), 1.81 (s, 6H; CH_3). ^{13}C NMR (75 MHz, $CDCl_3$): δ = 160.1, 143.9, 139.3, 135.2, 134.7, 132.9, 127.6, 127.1, 120.2 (2C; 8/8′-*C*H), 13.3 (br s, 2C; 5/5′-CCH_3), 10.0, 9.8, 9.6 (d, J = 6 Hz, 2C; 2/2′-CCH_3), 9.1. ^{19}F NMR (376 MHz, CD_2Cl_2): δ = −141.0 (dq, J_{FF} = 105 Hz, J_{FB} = 33 Hz, 2F; 2 × B*F*F), −147.4 (m, 2F; 2 × BF*F*). ^{11}B NMR (128 MHz, CD_2Cl_2): δ = 0.34 (dd, J_{FB} = J_{BF} = 33 Hz, 2B; 2 × BF_2). HRMS (ESI+): *m*/*z* calcd. for $C_{28}H_{32}B_2F_4N_4Na$ $[M+Na]^+$: 545.2641; found: 545.2551.

2.2. Electrochemical Characterization. *2.2.1. Chemicals.* Electrochemical grade dichloromethane (DCM) and ferrocene obtained from Aldrich Chemical Co (Milwaukee, WI) were used without further purification. Supporting electrolyte, tetra-*n*-butyl-ammonium hexafluorophosphate ($TBAPF_6$) was obtained from Fluka.

2.2.2. Apparatus and Methods. Absorption and fluorescence measurements were made in DCM in air. The absorbance measurements were carried out with a DU640 spectrophotometer (Beckman, Fullerton, CA) with a 1 cm cell. Fluorescence measurements were carried out on a double beam QuantaMaster Spectrofluorimeter (Photon Technology International, Birmingham, NJ) with a 70 W Xe lamp as the excitation source and slit width of 0.5 mm. The quantum yield was calculated using fluorescein as a standard. Three electrode cell configurations were used for all electrochemistry experiments. A platinum disk working electrode with an area of 0.0314 cm^2 inlaid in glass was used for all cyclic voltammetry and chronoamperometry measurements. An electrode bent at 90° was used for the ECL experiments. Platinum and silver wires were used as counter and reference electrodes, respectively. Platinum working electrodes were polished with 0.3 μm alumina for several min and then sonicated in ethanol and water for 5 min. All glassware was dried at 120 °C for 2 h prior to transfer to the helium atmosphere glovebox (Vacuum Atmospheres Corp., Hawthorne, CA). Solutions for all electrochemical and ECL measurements were prepared inside the glovebox and sealed in a cell closed with a Teflon cap to allow measurements outside the glovebox. Cyclic voltammograms were calibrated using ferrocene as a standard taking its potential as 0.342 V vs SCE.[41] The electrode area was determined by chroamperometry measurements with 2 mM ferrocene in DCM assuming a diffusion coefficient (D) of 1.2 × 10^{-5} cm^2/s. The diffusion coefficient values of the dyes were determined by the scan rate (v) dependences from the Randles-Ševčik equation and chroamperometric pulsing for 1 s from the Cottrell equation. ECL spectra were generated by alternate potential steps to 80 mV past the peaks for the first reduction and oxidation waves. The frequency of pulsing was 10 Hz and the time was 2 min. ECL emission spectra were recorded with a Princeton Instruments Spec 10 CCD camera (Trenton, NJ) with an Acton SpectrPro-150 monochromator. The CCD camera was cooled to −100 °C with liquid nitrogen. A Hg/Ar pen-ray lamp (Oriel, Stratford, CT) was used to calibrate the wavelengths. Relative ECL quantum yields were determined by potential step experiments and comparing the intensity of the ECL with results for the $Ru(bpy)_3^{2+}$ under similar conditions.

3. RESULTS AND DISCUSSION

3.1. Chemical Dimerization. After detailed investigations for oxidative coupling of not fully substituted BODIPYs, one method was found, which seems to be promising. The α-unsubstituted BODIPY **1**(×3,8) is dimerized with anhydrous $FeCl_3$[42,43] in CH_2Cl_2 at 0 °C to the 3,3′-dimer (Scheme 3). Addition of two equivalents of $FeCl_3$ under stirring causes a change of the orange

Scheme 3. Chemical and Electrochemical Dimerization of 1(×3,8) Monomer to 3,3-Dimer

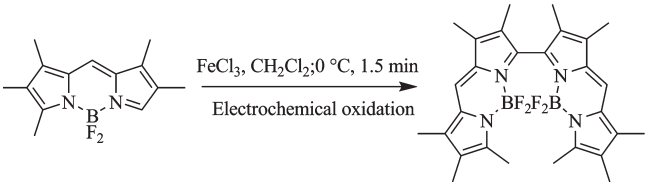

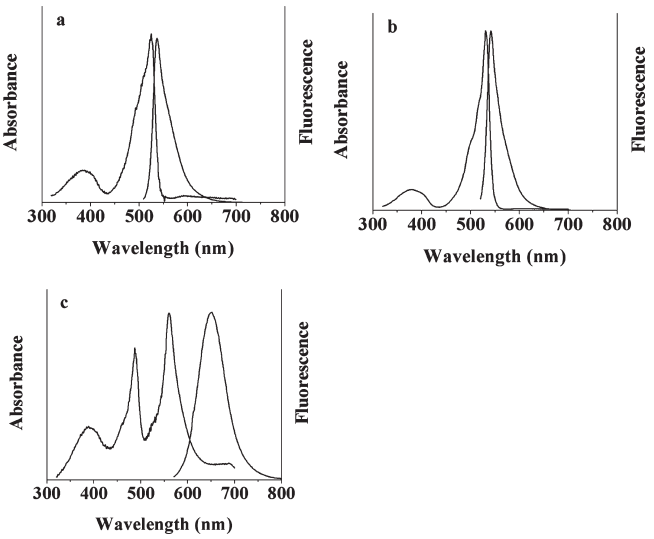

Figure 1. Absorption and fluorescence spectra of 2 μM BODIPY dyes in dichloromethane: (a) **1**(×3,8); (b) **2**(×8); (c) 3,3′-dimer.

1(×3,8) monomer into the deep red 3,3′-dimer. The reaction is quenched after 1.5 min by addition of methanol to prevent decomposition which may cause the reaction mixture to turn green after approximately 5 min. Quenching by methanol allows one to isolate the 3,3′-dimer in a yield of 50% with 49% percent still remaining as **1**(×3,8). The above-mentioned reaction conditions are so far the best for the oxidative coupling of **1**(×3,8). The product 3,3′-dimer shows all the same characteristics in the spectroscopic and photophysical studies as the earlier described BODIPY dimers obtained by 2-fold complexation of bidipyrrin ligands.[44,45] If the *meso*-unsubstituted hexamethyl BODIPY **2**(×8) is subjected to the same conditions (2 equiv of $FeCl_3$ in CH_2Cl_2), almost no decomposition or reaction can be observed after several days. Conditions for chemical dimerization proposed in this paper are drastically different from those used for the dimerization of BODIPY dyes through positions 2 and 6, where room temperature was applied in the presence of $FeCl_3$.[18]

3.2. Photophysical Studies. The UV−vis absorption behavior of the **1**(×3,8) monomer is shown in Figure 1a and Table 1. The behavior is characteristic of a simple BODIPY monomer with two absorption maxima at 383 and 524 nm, which correspond to the S2−S0 and S1−S0 transitions, with the fluorescence maximum at 537 nm.

The Stokes shift for the **1**(×3,8) monomer is small, which is characteristic of BODIPY monomers.[1,6,7] The **2**(×8) showed similar behavior with a slightly red-shifted wavelength for absorption and fluorescence due to the presence of the additional methyl group at position 3 (Figure 1b). The 3,3′-dimer shows

Table 1. Spectroscopy Properties of the Studied BODIPY Dyes

dye	λ_{max}(abs) (nm)	λ_{max}(fluor) (nm)	$\varepsilon(10^4\ M^{-1}cm^{-1})$	Φ_{fluor}	E_s (eV)
1(x3,8)	383, 524	537	0.9, 8.8	1.0	2.30
2(x8)	380, 529	541	1.0, 8.9	1.0	2.29
3,3′-dimer	387, 489, 562	650	1.66, 6.44, 7.36	0.7	1.91

characteristic excitonic splitting of the absorption spectra with one lower and one higher energetic process (Figure 1c),[44,45] producing three absorption features at 387, 489, and 562 nm. The dimer also shows a larger Stokes shift with the fluorescence maximum at 650 nm. The quantum yield for the dimer is smaller than that of the monomer because of splitting of excited state leading to an increase in intersystem crossing and nonradiative decay. The results obtained here are close to the photophysical results for the dimers obtained for 2-fold BF_2 coordination of the free-base ligands.[44,45]

3.3. Electrochemical Studies. Two general principles govern the electrochemical behavior of BODIPY compounds. First, the α and β sites are subject to electrophilic and nucleophilic attack, so substitution of these positions serves to stabilize the radical ions. Second, second reduction and oxidation waves (i.e., from the radical ion to the dianion) involve a much greater potential difference (>1 V) than in aromatic hydrocarbons and most heterocycles, so, in fact, multiple peaks are rarely seen within the solvent window for species with stable radical ions.[17] Thus, the CV of **1**(×3,8) indicates some instability on reduction because of the absence of the substituent in the 3 and 8-positions (Figure 2). The reduction peak for this compound, at −1.32 V, is close to that of other BODIPY dyes that emit at similar wavelengths. Further, the chemical irreversibility of the first anodic peak (at 1.12 V) and the appearance of the two peaks on oxidation suggest a follow-up reaction of the radical cation to produce a species that is oxidized in a separate wave.

As discussed below we suggest the follow-up reaction is formation of the dimer on oxidation of **1**(×3,8), where the oxidation peak at 1.57 V is assigned to oxidation of the dimer.

In contrast to the CV results for **1**(×3,8), **2**(×8) shows a more chemically reversible reduction at −1.30 V (close to that of **1**(×3,8)) and quasi-reversible oxidation at 1.11 V (Figure 3). Experiments and digital simulations[46] show a high degree of reversibility for reduction at scan rates of 1 and 0.5 V/s with deviation at $v \leq 0.25$ V/s. This suggests a following reaction that might be responsible for an unknown species producing the anodic wave on reversal at −0.4 V. Digital simulations confirm the nernstian behavior for the oxidation over a range of scan rates (0.1 to 1 V/s) (Supporting Information Figure S1). The rate constant for the dimerization of **1**(×3,8) can be determined by using digital simulations and fitting them to the experimental curve (Supporting Information Figure S2). The redox potentials from the CV studies of the **1**(×3,8) and **2**(×8) species can be used in simulations as they correspond with the potentials of the monomer and the dimer. The radical cation-radical cation (rcrc) mechanism[35,47] was taken for the simulation mechanism; the alternative cation-substrate coupling showed larger deviations from the experimental data. The dimerization mechanism is thus:

$$R-H_2 \rightarrow R-H_2{}^{\cdot+} + e \quad (1)$$

$$R-H_2{}^{\cdot+} + R-H_2{}^{\cdot+} + H_2R-RH_2{}^{2+} \quad (2)$$

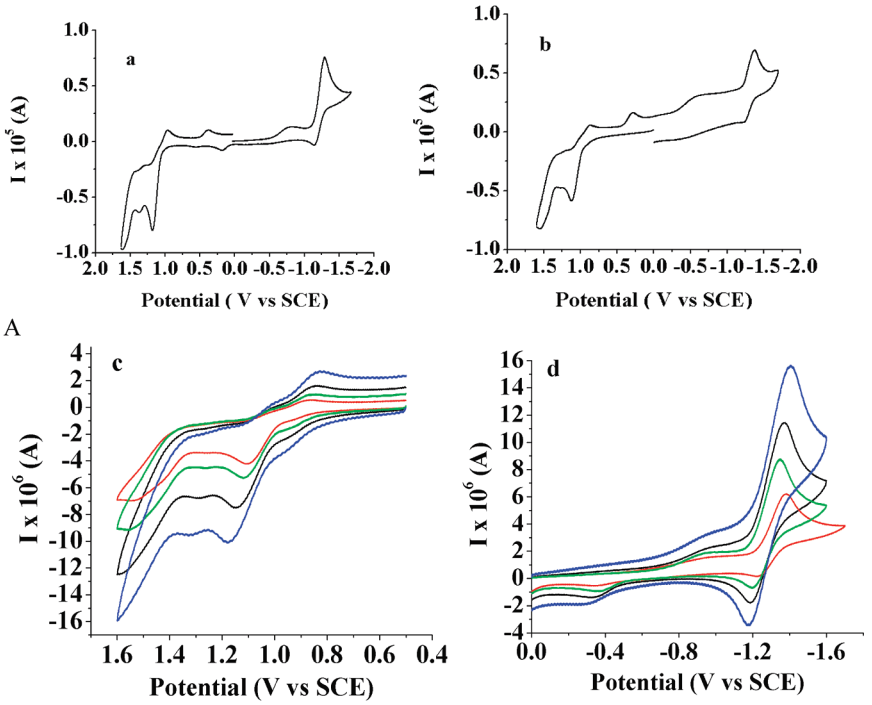

Figure 2. Cyclic voltammogram of 1.5 mM **1**(×3,8) at a scan rate of 0.1 V/s in dichloromethane at platinum working electrode (area = 0.0314 cm^2); supporting electrolyte: 0.1 M $TBAPF_6$; (a) forward scan to the negative direction; (b) forward scan to the positive direction; scan rate dependence for oxidation (c) and reduction (d). Scan rates of 0.1 V/s (red line); 0.25 V/s (green line); 0.5 V/s (black line); 1 V/s (blue line) were used.

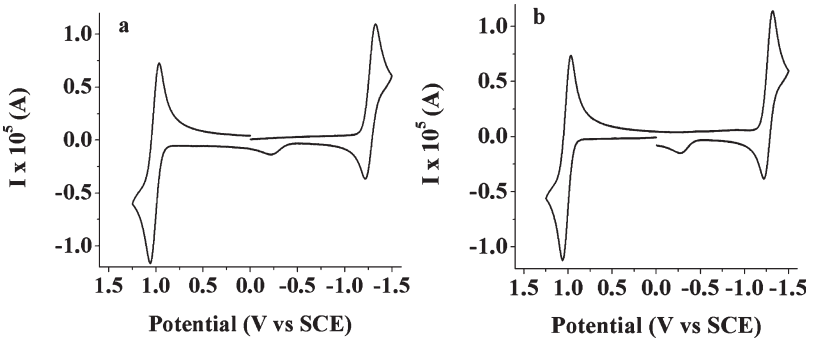

Figure 3. Cyclic voltammogram of 1.5 mM **2**(x8) at a scan rate of 0.1 V/s in dichloromethane at platinum working electrode (area = 0.0314 cm^2); supporting electrolyte: 0.1 M $TBAPF_6$; (a) forward scan to the negative direction; (b) forward scan to the positive direction.

$$H_2R - RH_2^{2+} + HR - RH + 2H^+(\text{fast}) \quad (3)$$

$$HR - RH \rightarrow HR - RH^{\cdot +} + e \quad (4)$$

$$HR - RH^{\cdot +} \rightarrow HR - RH^{2+} + e \quad (5)$$

The best fit was obtained for a second order dimerization rate constant of 4×10^4 $M^{-1}s^{-1}$. Simulations were done for two concentrations, providing evidence for the second order nature of the reaction and the reliability of calculations. The dimerization constant obtained in this case is significantly larger that for dimerization through positions 2,6, which is in the range of 400−2000 M^{-1} s^{-1}.[17,18] This conclusion corresponds fairly well with the chemical dimerization procedure and much faster dimerization rate.

The CV of the chemically synthesized 3,3′-dimer, shown in Figure 4, indicates oxidation (Figure 4c) with a chemically reversible peak at 1.0 V and less reversible one at 1.5 V. The reduction of the dimer (Figure 4d) shows two peaks at −1.23 and −1.6 V that are less reversible. The irreversibility of the first peak confirms the importance of the presence of substitution in the *meso*-position on the stability of the radical anion. The reduction current (Figure 4c,d) varies with the square root of scan rate, thus excluding a significant influence of adsorption or other surface processes. The existence of two reduction and oxidation waves with the 3,3′-dimer suggests that the possibility of greater delocalization across the two units allowing closer spacing of the second electron transfer waves than seen for the monomer.

3.4. Electrogenerated Chemiluminescence. The ECL spectra resulting from the annihilation reaction between the **1**(×3,8) radical anion and radical cation are shown in Figure 5(a−d). These can be compared to the ECL from **2**(×8), which showed the formation of one ECL peak at 565 nm corresponding to the

dx.doi.org/10.1021/ja207545t |*J. Am. Chem. Soc.* 2011, 133, 19498–19504

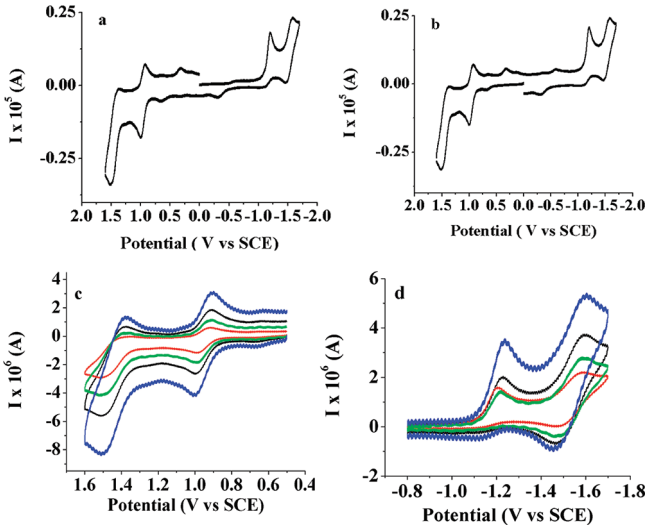

Figure 4. Cyclic voltammograms of 0.7 mM 3,3′-dimer at a scan rate of 0.1 V/s in dichloromethane at platinum working electrode (area = 0.0314 cm^2); supporting electrolyte: 0.1 M $TBAPF_6$; (a) forward scan to the negative direction; (b) forward scan to the positive direction; scan rate dependence for (c) oxidation and (d) reduction. Scan rates of 0.1 V/s (green line); 0.25 V/s (red line); 0.5 V/s (black line) and 1 V/s (blue line) were used.

wavelength of monomer emission (Figure 5e). Most other BODIPY species show this kind of emission agreeing with the PL. The offset between the PL and ECL emission results from an inner filter effect (self-absorption) in ECL at the relatively high concentration used for ECL compared to that for PL studies, as well as a small difference between the different instruments used for PL and ECL studies. With **1**(×3,8) there is also long wavelength emission at 656 nm, considerably red-shifted from the smaller monomer emission peak at 560 nm. This longer wavelength emission correlates quite well with the ECL seen from the 3,3′-dimer itself at 679 nm, and its PL (Figure 5f). The overall ECL intensity for the monomer decreased during consecutive stepping at longer times, because of the dimerization reaction and also a slower reaction of the radical anion because of the unsubstituted 8-position. This unsubstituted 8-position also causes decay of the dimer signal. At long times the shorter wavelength (monomer) peak was larger than the longer wavelength (dimer) one, because of the relative instability of the two species.

The chemically synthesized 3,3′-dimer showed one ECL peak at 679 nm near the observed PL emission (Figure 5f). The long wavelength ECL signal at 656 found with **1**(×3,8) correlates quite well with the ECL for the chemically synthesized dimer at 679 nm, thus providing strong evidence for the electrochemical formation of the dimer (Figure 5g). This also corresponds to the appearance of a second oxidation peak in the cyclic voltammograms.

The results here show the importance of the nature of substitution position on the electrochemical properties. Lack of substitution in position 3 promotes the dimerization reaction while position 8 affects mostly protonation on reduction which affects the reversibility of the electrochemical process and the stability of the radical anions. The mechanism of the emission of the dimer during ECL is proposed to be:

$$1(\times 3,8) + e^- \rightarrow 1(\times 3,8)\cdot^- \quad (6)$$

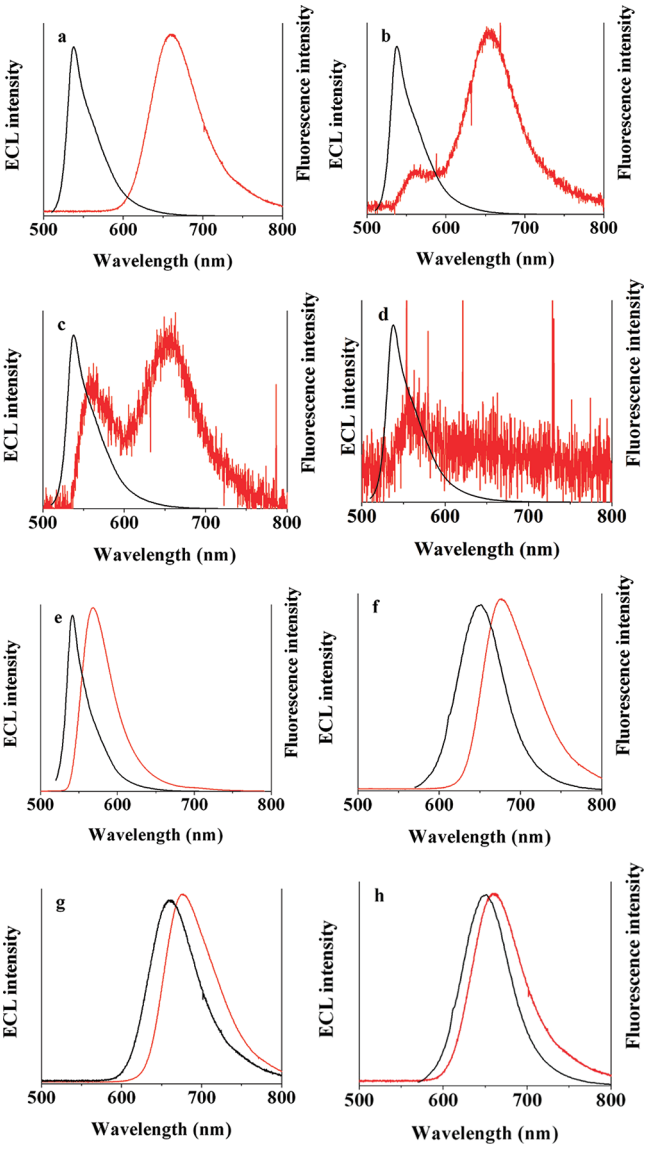

Figure 5. (a–d) ECL spectra for 1.5 mM (red line) and fluorescence spectra for 2 μM (black line) of the **1**(×3,8) in dichloromethane. ECL spectra were generated by pulsing potential at a frequency from −1.4 to 1.2 V for different times (min): (a) 2; (b) 4; (c) 6; (d) 8; (e) ECL (red line) and fluorescence spectra (black line) for 2 μM **2**(×8) with stepping from −1.38 to 1.19 V for 2 min; (f) ECL spectra for 0.7 mM (red line) and fluorescence spectra for 2 μM (black line) of 3,3′-dimer. ECL spectra were generated by stepping potential from −1.68 to 1.08 V; (g) comparison of the ECL spectra of 1.5 mM 1×3,8 (red line) and 0.7 mM 3,3′-dimer (black line); (h) comparison of the ECL spectra of 1.5 mM 1×3,8 (red line) and fluorescence spectra of 2 μM 3,3′-dimer (black line). Frequency of pulsing 10 Hz; platinum electrode with an area equal to 0.0314 cm^2 and 0.1 M $TBAPF_6$ supporting electrolyte were used for all electrochemistry measurements.

$$1(\times 3,8) - e^- \rightarrow 1(\times 3,8)\cdot^+ \quad (7)$$

$$1(\times 3,8)\cdot^+ + 1(\times 3,8)\cdot^+ \rightarrow 3,3' - \text{dimer} - H_2{}^{2+} \quad (8)$$

$$3,3' - \text{dimer} - H_2{}^{2+} \rightarrow 3,3' - \text{dimer} + 2H^+ \quad (9)$$

dx.doi.org/10.1021/ja207545t |J. Am. Chem. Soc. 2011, 133, 19498–19504

Table 2. Electrochemical Properties of the BODIPY Dyes

	E_p (V vs SCE)					
dye	A/A^-	A/A^+	λ_{max} (ECL) (nm)	Φ_{ECL}[a]	ΔH_{ann} (eV)	D (cm^2/s)
1(×3,8)	−1.32	1.12	560	0.005	2.28	6.8×10^{-6}
		1.57	656			
2(×8)	−1.30	1.11	565	0.008	2.25	6.6×10^{-6}
3,3′-dimer	−1.23	1.00	679	0.004	2.07	5.2×10^{-6}
	−1.60	1.50				

[a] Relative to $Ru(bpy)_3^{2+}$ (taken as unity).

$$3,3' - \text{dimer} - e^- \rightarrow 3,3' - \text{dimer}^{\cdot +} \quad (10)$$

$$1(\times 3,8)^{\cdot -} + 3,3' - \text{dimer}^{\cdot +} \rightarrow 1(\times 3,8) + 3,3' - \text{dimer}^* \quad (11)$$

$$3,3' - \text{dimer}^* \rightarrow 3,3' - \text{dimer} + h\upsilon \quad (12)$$

The enthalpy of annihilation can be estimated from the thermodynamic parameters: $\Delta G_{ann} = \Delta H_{ann} - T\Delta S$, where ΔG_{ann} is obtained from the estimated E^o values and an entropic term approximately equal to 0.1 eV. The process goes through the singlet state if the electrochemical energy is larger than the excited state energy needed to produce singlet state (E_s) (Tables 1 and 2). The results for the energy of annihilation and energy needed for ECL are fairly close for the **1**(×3,8), **2**(×8) and 3,3′-dimer needed for singlet state (S-route) process.

4. CONCLUSIONS

Chemical and electrochemical dimerization of the BODIPY species **1**(×3,8) was carried out. Lack of substitution on position 3 was important for the electrochemical dimerization with the absence of dimerization or other bond formation at position 8. Chemical dimerization was achieved with $FeCl_3$ as an oxidative coupling reagent, consistent with the electrochemical route, demonstrated by CV and ECL, through the radical cation.

■ ASSOCIATED CONTENT

Supporting Information. Additional CVs NMR and ESI MS data. This material is available free of charge via the Internet at http://pubs.acs.org.

■ AUTHOR INFORMATION

Corresponding Author
ajbard@mail.utexas.edu

■ ACKNOWLEDGMENT

We thank the Center for Electrochemistry, Roche Diagnostics, Inc., and the Robert A. Welch Foundation (F-0021) and Deutsche Forschungsgemeinschaft (DFG) for support of this research.

■ REFERENCES

(1) Loudet, A.; Burgess, K. *Chem. Rev.* **2007**, *107*, 4891–4932.
(2) Urano, Y.; Asanuma, D.; Hama, Y.; Koyama, Y.; Barrett, T.; Kamiya, M.; Nagano, T.; Watanabe, T.; Hasegawa, A.; Choyke, P. L.; Kobayashi, H. *Nat. Med.* **2008**, *15*, 104–109.
(3) Bouit, P. A.; Kamada, K.; Feneyrou, P.; Berginc, G.; Toupet, L.; Maury, O.; Andraud, C. *Adv. Mater.* **2009**, *21*, 1151–1154.
(4) Golovkova, T. A.; Kozlov, D. V.; Neckers, D. C. *J. Org. Chem.* **2005**, *70*, 5545–5549.
(5) Rousseau, T.; Cravino, A.; Bura, T.; Ulrich, G.; Ziessel, R.; Roncali, J. *Chem. Commun.* **2009**, *13*, 1673–1675.
(6) Lai, R. Y.; Bard, A. J. *J. Phys. Chem. B* **2003**, *107*, 5036–5042.
(7) Sartin, M. M.; Camerel, F.; Ziessel, R.; Bard, A. J. *J. Phys. Chem. C* **2008**, *112*, 10833–10841.
(8) Kollmannsberger, M.; Garries, T.; Heinl, S.; Breu, J.; Daub, J. *Angew. Chem., Int. Ed.* **1997**, *36*, 1333–1335.
(9) Trieflenger, C.; Röhr, H.; Rurack, K.; Daub, J. *Angew. Chem., Int. Ed.* **2005**, *44*, 6943–6947.
(10) Röhr, H.; Trieflenger, C.; Rurack, K.; Daub, J. *Chem.—Eur. J.* **2006**, *12*, 689–700.
(11) Goze, C.; Ulrich, G.; Mallon, L. J.; Allen, B. D.; Harriman, A.; Ziessel, R. *J. Am. Chem. Soc.* **2006**, *128*, 10231–10239.
(12) Chen, J.; Burghart, A.; Derecskei-Kovacs, A.; Burgess, K. *J. Org. Chem.* **2000**, *65*, 2900–2906.
(13) Nepomnyashchii, A. B.; Bröring, M.; Ahrens, J.; Krüger, R.; Bard, A. J. *J. Phys. Chem. C.* **2010**, *114*, 14453–14460.
(14) Seidel, D.; Lynch, V.; Sessler, J. L. *Angew. Chem., Int. Ed.* **2002**, *41*, 1422–1425.
(15) Köhler, T.; Seidel, D.; Lynch, V.; Arp, F. O.; Ou, Z.; Kadish, K. M.; Sessler, J. L. *J. Am. Chem. Soc.* **2003**, *125*, 6872–6873.
(16) Richter, T. D.; Lash, T. D. *J. Org. Chem.* **2004**, *69*, 8842–8850.
(17) Nepomnyashchii, A. B.; Cho, S.; Rossky, P. J.; Bard, A. J. *J. Am. Chem. Soc.* **2010**, *132*, 17550–17559.
(18) Nepomnyashchii, A. B.; Bröring, M.; Ahrens, J.; Bard, A. J. *J. Am. Chem. Soc.* **2011**, *133*, 8633–8645.
(19) Yoshida, K. Electrooxidation in Organic Chemistry. *The Role of Cation Radicals as Synthetic Intermediates*; John Wiley and Sons: New York, 1984.
(20) Kyriacou, D. *Modern Electroorganic Chemistry*; Springer-Verlag: Berlin, 1994.
(21) Shono, T. *Electroorganic Synthesis*; Academic Press: London, 1991.
(22) Baizer, M. M. *In Organic Electrochemistry*; Baizer, M. M., Lund, H., Eds.; Marcel Dekker: New York, 1983; Chapter 20.
(23) Baizer, M. M.; Petrovich, J. P. In *Progress in Physical Organic Chemistry*; Streitwieser, A., Taft, R. W., Eds.; Interscience: New York, 1970; Vol. 7, p 189−227.
(24) Baizer, M. M. *J. Electrochem. Soc.* **1964**, *111*, 215–222.
(25) Bobbitt, J. M.; Noguchi, I.; Yagi, H.; Weisgraber, K. H. *J. Org. Chem.* **1976**, *41*, 845–850.
(26) Gallardo, I.; Guirado, G.; Marquet, J.; Vila, N. *Angew. Chem., Int. Ed.* **2007**, *46*, 1321–1325.
(27) Goldberg, I. B.; Boyd, D.; Hirasawa, R.; Bard, A. J. *J. Phys. Chem.* **1974**, *78*, 295–299.
(28) Berti, C.; Greci, L.; Andruzzi, R.; Trazza, A. *J. Org. Chem.* **1985**, *50*, 368–373.
(29) Tsuchida, E.; Yamamoto, K.; Oyaizu, K.; Iwasaki, N.; Anson, F. C. *Inorg. Chem.* **1994**, *33*, 1056–1063.
(30) Macias-Ruvalcaba, N. A.; Evans, D. H. *J. Phys. Chem. C* **2007**, *111*, 5805–5811.
(31) Costentin, C.; Saveant, J. M. *J. Phys. Chem. A* **2005**, *109*, 4125–4132.
(32) Zhou, F.; Bard, A. J. *J. Am. Chem. Soc.* **1994**, *116*, 393–394.
(33) Treichel, D. A.; Mirkin, M. V.; Bard, A. J. *J. Phys. Chem.* **1994**, *98*, 5751–5757.
(34) Debad, J. D.; Morris, J. C.; Lynch, V.; Magnus, P.; Bard, A. J. *J. Am. Chem. Soc.* **1996**, *118*, 2374–2379.
(35) Debad, J. D.; Morris, J. C.; Magnus, P.; Bard, A. J. *J. Org. Chem.* **1997**, *62*, 530–537.
(36) Fabrizio, E. F.; Prieto, I.; Bard, A. J. *J. Am. Chem. Soc.* **2000**, *122*, 4996–4997.

(37) Lee, S. K.; Richter, M. M.; Strekowski, L.; Bard, A. J. *Anal. Chem.* **1997**, *69*, 4126–4133.
(38) For reviews on ECL, see: (a) Bard, A. J. *Electrogenerated Chemiluminescence*; Marcel Dekker: New York, 2004. Richter, M. M. *Chem. Rev.* **2004**, *104*, 3003–3036. (b) Miao, W. *Chem. Rev.* **2008**, *108*, 2506–2553.
(39) Vos de Wael, E.; Pardoen, J. A.; Van Koeveringe, J. A.; Lugtenburg, J. *Recl. Trav. Chim. Pays-Bas* **1977**, *96*, 306–309.
(40) Semeikin, A. S.; Berezin, M. B.; Chernova, O. M.; Antina, E. V.; Syrbu, S. A.; Lyubimova, T. V.; Kutepov, A. M. *Russ. Chem. Bull., Int. Ed.* **2003**, *52*, 1807–1813.
(41) Sahami, S.; Weaver, M. *J. Electroanal. Chem.* **1981**, *122*, 155–170.
(42) Bolm, C.; Legros, J.; Le Paih, J.; Zani, L. *Chem. Rev.* **2003**, *104*, 6217–6254.
(43) Diaz, D. D.; Miranda, P. O.; Padron, J. I.; Martin, V. S. *Curr. Org. Chem.* **2006**, *10*, 457–476.
(44) Bröring, M.; Krüger, R.; Link, S.; Kleeberg, C.; Köhler, S.; Xie, X.; Ventura, B.; Flamigni, L. *Chem.—Eur. J.* **2008**, *14*, 2976–2983.
(45) Ventura, B.; Marconi, G.; Bröring, M.; Krüger, R.; Flamigni, L. *New J. Chem.* **2009**, *33*, 428–438.
(46) (a) Rudolph, M. *J. Electroanal. Chem.* **1991**, *314*, 13–22. (b) Rudolph, M. *J. Electroanal. Chem.* **1992**, *338*, 85–98. (c) Feldberg, S. W.; Goldstein, C. I.; Rudolph, M. *J. Electroanal. Chem.* **1996**, *413*, 25–36.
(47) Nadjo, L.; Saveant, J. M. *J. Electroanal. Chem.* **1973**, *44* 327–366.